CHEMISTRY & SUSTAINABILITY

CHEMSUSCHEM

ENERGY & MATERIALS

Accepted Article

Title: Oxidative Methane Conversion to Ethane on Highly Oxidized Pd/CeO2 Catalysts Below 400 ˚C

Authors: Gihun Kwon, Dongjae Shin, Hojin Jeong, Suman Kalyan Sahoo, Jaeha Lee, Gunjoo Kim, Juhyuk Choi, Do Heui Kim, Jeong Woo Han, and Hyunjoo Lee

To be cited as: *ChemSusChem* 10.1002/cssc.201903311

Link to VoR: http://dx.doi.org/10.1002/cssc.201903311

A Journal of

ChemPubSoc Europe

WILEY-VCH

www.chemsuschem.org

10.1002/cssc.201903311

WILEY-VCH

COMMUNICATION

Oxidative Methane Conversion to Ethane on Highly Oxidized Pd/CeO_2 Catalysts Below 400 ˚C

Gihun Kwon†[a], Dongjae Shin†[b], Hojin Jeong[a], Suman Kalyan Sahoo[b], Jaeha Lee[c], Gunjoo Kim[a], Juhyuk Choi[a], Do Heui Kim[c], Jeong Woo Han*[b] and Hyunjoo Lee*[a]

Abstract: Methane upgrading into more valuable chemicals has received much attention. Herein, we report oxidative methane conversion to ethane using gaseous O_2 at low temperatures (< 400 ˚C) and atmospheric pressure in a continuous reactor. A highly oxidized Pd deposited on ceria could produce ethane with the productivity as high as 0.84 mmol g_{cat}^{-1} h^{-1}. The Pd-O-Pd sites, not Pd-O-Ce, were the active sites for the selective ethane production at low temperatures. Density functional theory calculations confirmed that Pd-O-Pd site is energetically more advantageous for C-C coupling whereas Pd-O-Ce prefers CH_4 dehydrogenation. The ceria helped Pd maintain highly oxidic state despite reductive CH_4 flow. This work can provide new insight for methane upgrading into C2 species.

Direct conversion of methane to value-added chemicals such as olefins, aromatics, and methanol has recently received much attention due to the depletion of crude oil and the large reserves of shale gas.[1] The methane is often emitted from shale gas mines into air, causing a severe greenhouse effect. The majority of methane is burned, also producing a significant amount of carbon dioxide. Converting the methane into more valuable chemicals would be beneficial for not only producing more benefits but also for protecting environment. However, direct conversion is very difficult because the first C-H bond activation requires high energy (439 kJ/mol).[2] The inertness of methane hinders the selective production of valuable chemicals and instead the methane conversion often results in over-oxidation to CO_2 or severe coke formation.[3]

Despite the difficulties, oxidative or non-oxidative methane conversion has been reported. The oxidative conversion uses oxidants such as H_2O_2 or O_2, typically allowing milder reaction conditions.[4] Methanol could be directly produced from methane using H_2O_2 as an oxidant, however, a batch reactor was typically used and H_2O_2 is more expensive than methanol, making its practical application improbable. Ethylene could be produced using O_2 in a continuous reactor, but the reaction temperature is typically higher than 700 ˚C, and various side-products were formed together due to its radical-derived chemistry,[5] causing higher cost for separation.[6] Methanol was produced from a continuous flow reactor using O_2, but the productivity was very low as 0.02 mmol g_{cat}^{-1} h^{-1}.[4a, 4c] The non-oxidative conversion uses methane only, but it typically require very high temperature (> 1000 ˚C). Selective production of olefin or benzene have been reported,[7] but these results were not easily reproduced.

Using a continuous flow reactor is preferred for the direct methane conversion. O_2 as an oxidant, instead of H_2O_2 or N_2O, is preferred for the oxidative methane conversion.[1b, 2, 8] Because conventional oxidative coupling of methane generates radicals at high temperatures of >700 ˚C resulting in various side-products, the catalysts enabling surface reaction at much lower temperatures are desired.

We show here that highly oxidized Pd/CeO_2 catalysts can catalyze oxidative methane upgrading into ethane at low temperatures using gaseous O_2. The studies on methane coupling at low temperatures below 400 ˚C are rare. Pt/SiO_2 or Pd/Al_2O_3 have been used for methane coupling below 400 ˚C but they could not complete a catalytic cycle; after flowing methane, hydrogen gas was required to extract the adsorbed products from the catalyst surface.[9] $(\equiv SiO)_2Ta$-H could have a closed catalytic cycle producing ethane continuously, but methane pressure was as high as 50 bar, and the ethane productivity was very low as 0.01 mmol g_{cat}^{-1} h^{-1} at 300 ˚C.[10] The detailed comparison for the catalysts producing ethane from methane at < 400 ˚C is provided in Table S1.

Pd/CeO_2 catalysts, on which Pd nanoparticles are dispersed on ceria surface, have been widely used for oxidations, such as CO oxidation, benzyl alcohol oxidation, and methane combustion.[11] The Pd surface can be easily oxidized and the formed PdO can behave as an oxidation catalyst.[12] The interface between Pd and ceria often behaves as efficient active sites for oxidation at lower temperatures.[3b, 13] Particularly, it was reported that Pd can be highly oxidized on ceria with a ratio of Pd to O smaller than 1.[14] Methane activation was also studied on Pd; the energy barrier was lower in PdO than metallic Pd.[15] Various Pd catalysts such as $Pd@CeO_2/Al_2O_3$ or Pd/ZSM-5 have been reported to be efficient for methane combustion.[3b, 16]

In this study, highly oxidized Pd/CeO_2 catalysts can catalyze the oxidative methane conversion producing ethane at low temperatures. The reaction kinetics were investigated by varying methane or O_2 partial pressure. Catalysts with different ratios of Pd-O-Pd and Pd-O-Ce sites were prepared and tested for ethane production. Density functional theory (DFT) calculations were performed to investigate the reaction mechanism on Pd-O-Pd and Pd-O-Ce sites.

† These authors equally contributed
[a] Gihun Kwon, Hojin Jeong, Gunjoo Kim, Juhyuk Choi, Hyunjoo Lee
Department of Chemical and Biomolecular Engineering
Korea Advanced Institute of Science and Technology
Daejeon 34141, South Korea
E-mail: azhyun@kaist.ac.kr
[b] Dongjae Shin, Suman Kalyan Sahoo, Jeong Woo Han
Department of Chemical Engineering
Pohang University of Science and Technology, Pohang
Gyeongbuk 37673, South Korea
E-mail: jwhan@postech.ac.kr
[c] Jaeha Lee, Do Heui Kim
School of Chemical and Biological Engineering
Institute of Chemical Processes, Seoul National University
Seoul, 08826, South Korea

Supporting information for this article is given via a link at the end of the document.

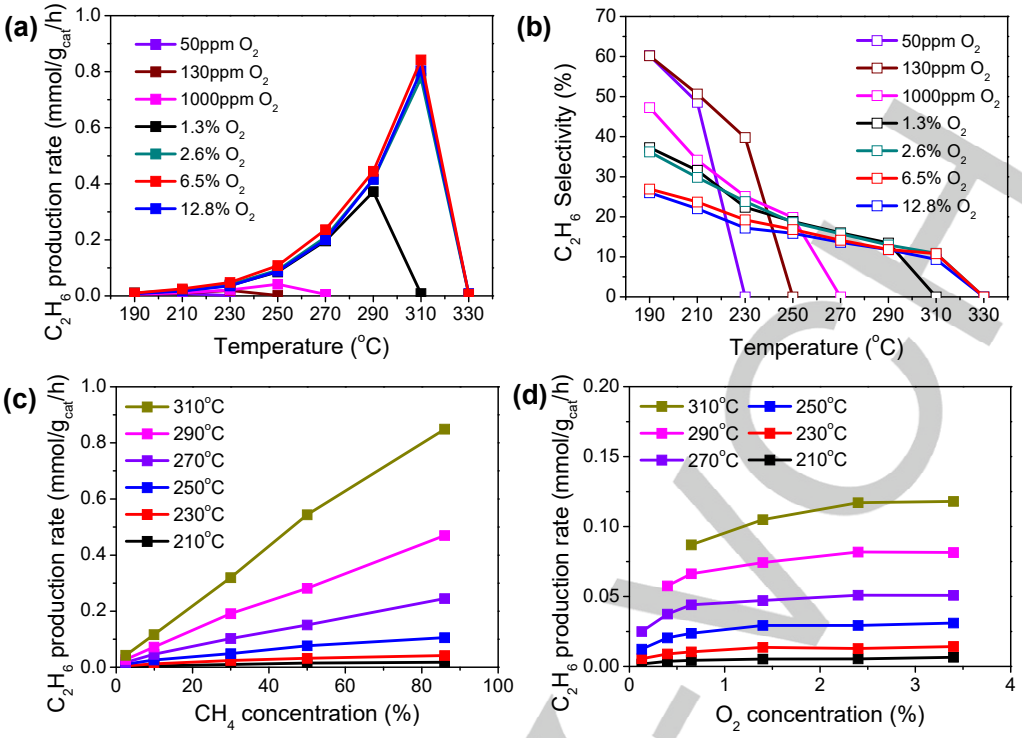

Figure 1. Effect of the temperature on the ethane (a) productivity and (b) selectivity with various O_2 contents. The CH_4 content was 86% with balance N_2 in (a) and (b). In the case of 12.8% O_2, 78% of CH_4 was used instead. Effect of the (c) CH_4 and (d) O_2 content. The O_2 content was 5% in (c), and the CH_4 content was 8.6% with balance N_2 in (d).

The highly oxidized Pd/CeO_2 catalyst was prepared by treating Pd/CeO_2, which was synthesized with a conventional deposition-precipitation, at 750 ˚C for 25 h under air. When a high concentration of CH_4 (86%) was flowed with gaseous O_2 (50 ppm ~ 6.5%) at elevated temperatures, C_2H_6 was produced with a productivity of 0.84 mmol g_{cat}^{-1} h^{-1} at 310 ˚C as shown in Figure 1a. The C_2H_6 selectivity was 11% at 310 ˚C with balance CO_2, and a trace amount of C_2H_4 was also detected with a productivity of 5 μmol g_{cat}^{-1} h^{-1}. When the temperature was 330 ˚C, the C_2H_6 production suddenly stopped. X-ray photoelectron spectroscopy (XPS) results showed that the Pd surface was reduced and extended X-ray absorption fine structure (EXAFS) result also showed that a strong Pd-Pd peak appeared after the reaction at 330 ˚C (Figure S1). This indicates that metallic Pd was not the active phase for methane coupling to produce ethane. The Pd catalyst after the reaction at 310 ˚C showed the same oxidic surface state as the fresh Pd catalyst. The C_2H_6 could be produced at 310 ˚C stably for 100 h (Figure S2).

As the O_2 content decreased, the highly oxidized Pd/CeO_2 catalyst was reduced at lower temperature, and then the ethane productivity dropped to nearly zero. Instead, the ethane selectivity was high; 60% of the ethane selectivity was observed at 190 ˚C and 50 ppm O_2 as shown in Figure 1b. When C_2H_6 was flowed with O_2, only 4.7 % of the C_2H_6 was converted to CO_2 at 310 ˚C (Figure S3). Only a small fraction of the produced C_2H_6 seems to be converted into CO_2. Various kinds of metals or metal oxide supports were tested. The C_2H_6 production was observed on Pd and Pt among Pd, Rh, Ru, Ir and Pt (Figure S4). The Pd had a much higher C_2H_6 productivity at lower temperatures than that of the Pt. When the Pd was deposited on ZrO_2, CeO_2, TiO_2 and SiO_2, the C_2H_6 production was observed in all cases, and the CeO_2 had the highest productivity and selectivity (Figure S5).

The effect of CH_4 and O_2 content was also examined. The C_2H_6 productivity increased linearly as CH_4 content increased as shown in Figure 1c. This trend was observed in a wide range of CH_4 content (2.5% ~ 86%) at various temperatures (210 ~ 310 ˚C), indicating that CH_4 activation can occur easily on the Pd/CeO_2 catalyst. On the other hand, the C_2H_6 productivity became saturated as O_2 content increased as shown in Figure 1d. The O_2 content at which the ethane productivity reached saturation increased at higher temperature; 1.4% at 210 ˚C to 2.4% at 310 ˚C. O_2 activation occurs more at higher temperature, resulting in higher C_2H_6 productivity. These results indicate that O_2 activation is more difficult. When O_2 content was low below 1%, the Pd/CeO_2 was reduced more easily, terminating the C_2H_6 production at lower temperatures. Facilitating O_2 activation while preventing the catalyst reduction is important to maximize the C_2H_6 production.

Whether the active site is Pd-O-Pd or Pd-O-Ce was investigated. Pd-O-Pd is the main bonding of PdO particles, and Pd-O-Ce is the site at the interface between Pd and CeO_2. The Pd-O-Ce is known to be efficient for methane combustion at lower temperatures.[3b, 13] The ratio of the surface Pd-O-Pd to Pd-O-Ce was varied by changing calcination temperatures. The 4 wt% Pd/CeO_2 was calcined at various temperatures to prepare the oxidic Pd catalysts with different degrees. XRD patterns and TEM images were shown in Figure S6 and S7. The Pd/CeO_2 calcined at 350, 550, 750 ˚C showed the XRD peak for CeO_2 only, while the Pd/CeO_2 calcined at 900 ˚C also showed the metallic Pd peaks. EDS mapping images show that Pd was well distributed on the CeO_2. The Pd domain size was 2.0, 2.3, 2.9, and 12.7 nm

for the Pd/CeO_2 catalysts calcined at 350, 550, 750, and 900 ˚C, respectively, when measured by CO chemisorption (Table S2). These catalysts were compared to commercial PdO with a Pd domain size of 17.8 nm. The oxidation state of surface Pd was estimated by XPS (Figure S8). In the Pd/CeO_2 catalysts, the oxidic Pd $3d_{5/2}$ peak appears at two different positions of 336.5 eV for Pd-O-Pd and 337.6 eV for Pd-O-Ce, while the metallic Pd $3d_{5/2}$ peak appears at 335.5 eV.[17] The oxidic XPS peaks were deconvoluted and the percentages of Pd-O-Pd or Pd-O-Ce at the surface were estimated from the peak area ratio in Figure S8. The surface of Pd/CeO_2 calcined at 900 ˚C was reduced after the calcination. As shown in Figure 2, the fraction of Pd-O-Pd sites increased from 30% to 41%, 50%, 58%, and 100% for the Pd/CeO_2 catalysts calcined at 350, 550, 750, 900 ˚C, and bulk PdO, respectively. EXAFS data in Figure S9 also confirmed that the peak for Pd-O-Pd increased while the peak for Pd-O-Ce decreased as the calcination temperature increased. Table S3 shows the fitting results of the EXAFS data. The coordination number for Pd-O-Pd increased from 2.3 to 3.3, 4.3, 5.3, and 8.0 in the Pd/CeO_2 calcined at 350, 550, 750, 900 ˚C, and bulk PdO, respectively. When C_2H_6 productivity was estimated per surface Pd atom, the turnover frequency becomes higher as the fraction of the Pd-O-Pd sites increase. Clearly, the Pd-O-Pd sites, not Pd-O-Ce, are the active sites for the methane coupling.

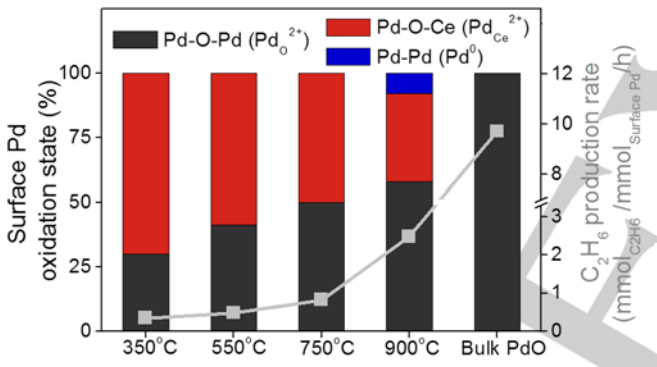

Figure 2. The ratios of the Pd-O-Pd and Pd-O-Ce estimated from XPS Pd 3d spectra (left axis) and turnover frequency for C_2H_6 production at 250˚C (right axis) on the Pd/CeO_2 catalysts calcined at 350, 550, 750, 900 ˚C, and bulk PdO. The number of surface Pd atom was estimated from CO uptakes.

DFT calculations were carried out to elucidate how Pd-O-Ce and Pd-O-Pd sites affect the oxidative methane coupling. Two models with Pd-O-Ce or Pd-O-Pd sites were constructed to understand the fundamental effects of these sites on the methane conversion. The partially embedded $Pd_7O_7/Ce_{33}O_{66}(111)$ surface (Figure S10c) was used as the Pd-O-Ce model; all the oxygens exposed on the PdO particle are Pd-O-Ce sites because all the oxygens (O1-O8) are neighbored by both Pd and Ce. The PdO(101) facet was used as the Pd-O-Pd model (Figure S10d); all the oxygens (O1-O2) are neighbored by Pd with Pd-O-Pd sites only. The computational details of constructing the models can be found in supporting information. The mechanistic steps of oxidative methane conversion considered in the DFT calculations are as follows:

(1) Adsorption of gas-phase CH_4 molecule (IS→E1)
(2) Dissociation of the adsorbed CH_4 (*CH_4) into *CH_3 and *H (E1→E2)
(3) Approach of two *CH_3 and two *H (E2→E3) or dissociation of *CH_3 into *CH_2 and *H (E2→E3-1)
(4) Coupling of two *CH_3 into *C_2H_6 (E3→E4)
(5) Formation of *H_2O with an O vacancy left on the surface (E4→E5)
(6) Desorption of *H_2O from the surface (E5→E6)
(7) Healing of O vacancy by gas-phase O_2 and desorption of *C_2H_6 (E6→FS)

The asterisk mark (*) denotes the chemical species adsorbed on the surface. Figure 3 shows the relative potential energies of each elementary step, and Figure S11 shows the optimized structures of each step and transition states. Table S4 shows the specific energy difference at each step. In the Pd-O-Ce model, the largest energy is required when the *H_2O is desorbed from the surface with the energy difference of 1.79 eV (step 6). In the Pd-O-Pd model, the largest energy is required when the *H_2O and oxygen vacancy are formed with the energy barrier of 1.40 eV (step 5). Since the barrier for rate-determining step (RDS) is smaller in the Pd-O-Pd model than that in the Pd-O-Ce model, the activity for the methane coupling would be higher in the Pd-O-Pd than that in the Pd-O-Ce, leading to the higher C_2H_6 productivity.

After *(CH_3+H) is formed from the dissociation of *CH_4 (step 2), the *CH_3 might be further dissociated into *(CH_2+H) (step 3-1). The reaction barrier of *CH_3 dissociation into *(CH_2+H) were compared. The barrier for the *CH_3 dissociation was 1.58 eV on the Pd-O-Pd model, while it was 1.07 eV on the Pd-O-Ce model. Especially, the *CH_3 dissociation (step 3-1) was energetically preferred to the pathway towards the coupling of two *CH_3 into *C_2H_6 (step 3) by 2.26 eV on the Pd-O-Ce model. However, the pathway to *C_2H_6 (step 3) was favored than the pathway to *CH_3 dissociation (step 3-1) by 0.29 eV on the Pd-O-Pd model. The Pd-O-Pd would produce C_2H_6 whereas the Pd-O-Ce would rather promote further dehydrogenation leading to the formation of CO_2.[18] The DFT results indicate that Pd-O-Pd sites can be the active sites producing C_2H_6 from methane, whereas Pd-O-Ce site would combust the methane.[3b, 13]

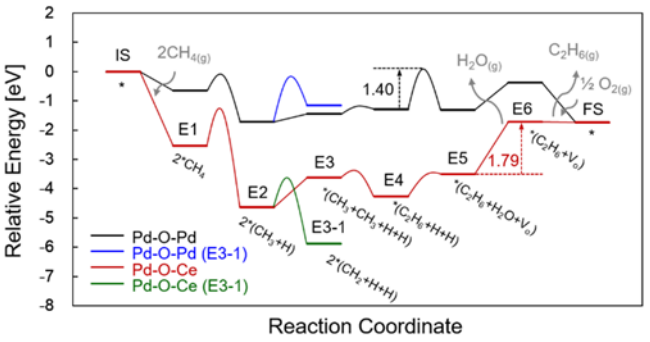

Figure 3. Reaction profiles of the oxidative methane conversion on Pd-O-Ce and Pd-O-Pd sites; the rate-determining steps were denoted using dashed arrows. The blue and green lines indicate the paths (E3-1) leading to CO_2 formation on Pd-O-Pd and Pd-O-Ce, respectively.

Although Pd-O-Pd are the active sites for the methane coupling, bulk PdO presented lower maximum C_2H_6 productivity and selectivity than the Pd/CeO_2 catalyst calcined at 750 ˚C

(Figure S12). H_2 temperature-programmed reduction (H_2-TPR) data showed that the bulk PdO was reduced at -17 ˚C whereas smaller Pd nanoparticles supported on CeO_2 was reduced at higher temperatures above 5 ˚C (Figure S13). The bulk PdO is reduced too easily while the Pd/CeO_2 can maintain the oxidic Pd state better in a high concentration of CH_4 flow. The oxidic Pd sites are the active sites for the methane coupling, and the ethane would not be produced in the presence of metallic Pd. The ceria support helped the Pd domain maintain the highly oxidized state in the reductive condition. The Pd/CeO_2 calcined at 350 ˚C or 550 ˚C showed a larger reduction peak than the other samples, indicating that more H_2 was consumed to reduce the surface with more Pd-O-Ce bonds.[19] O_2 temperature-programmed desorption (O_2-TPD) results also show that O_2 was desorbed more in the bulk PdO, causing more over-oxidation (Figure S14). The surface oxygen of the Pd/CeO_2 calcined at 750 ˚C started to be desorbed at the highest temperature, indicating that removing the oxygen from the catalyst surface is the most difficult. CH_4-TPR was also performed and the produced H_2O was detected using a mass spectrometer (Figure S15). The H_2O was detached from the Pd/CeO_2 calcined at 750 ˚C at the temperature similar to the bulk PdO, but the peak intensity was lower than that of bulk PdO. The H_2O was detached at higher temperatures from the Pd/CeO_2 calcined at 550 ˚C or 350 ˚C. In DFT calculations, the H_2O formation or desorption was identified as the most difficult step for methane coupling reaction on Pd-O-Pd or Pd-O-Ce model. H_2O could be detached at lower temperatures from the catalysts with more Pd-O-Pd sites, whereas H_2O was detached at higher temperatures from the catalysts with more Pd-O-Ce sites.

In summary, a highly oxidized Pd/CeO_2 catalyst could oxidize methane directly to ethane in a stable manner using gaseous O_2 below 400 ˚C. The Pd-O-Pd sites, not Pd-O-Ce, enabled the oxidative methane coupling. But the ceria helped Pd domain to maintain a highly oxidized state even under a high concentration of methane flow with higher C_2H_6 selectivity. DFT study confirmed that the C-C coupling can occur more on Pd-O-Pd site whereas Pd-O-Ce site would promote dehydrogenation into CO_2. This work opens up a new avenue to design heterogeneous catalysts for oxidative methane conversion into value-added chemicals at milder conditions.

Experimental Section

CeO_2 support was synthesized using a co-precipitation method. $Ce(NO_3)_3{\cdot}6H_2O$ (99.99%, Kanto chemical) 1.0 g was dissolved in 23.5 mL of deionized water under mild stirring. Aqueous ammonia (25~30% NH_4OH, Duksan) was injected dropwise until pH of the solution reached ~8.5. The resulting yellow slurry was filtered, and the obtained precipitate was dried and calcined at 500˚C for 5 h in air. Pd/CeO_2 was synthesized using a deposition-precipitation method. The CeO_2 powder 0.38 g was added in 5 mL deionized water. H_2PdCl_4 solution was prepared with 1: 2 molar ratio of $PdCl_2$ (99%, Sigma-Aldrich) to HCl (35~37%, Samchun) in deionized water. Na_2CO_3 solution was prepared by dissolving 0.53 g of Na_2CO_3 (99.999%, Sigma-Aldrich) in 10 mL of deionized water. The H_2PdCl_4 solution (~1 mL) containing 0.016 g Pd was added dropwise into the CeO_2 solution under rigorous stirring to prepare 4 wt% Pd/CeO_2 catalysts. The Na_2CO_3 solution was added together to control pH of the solution as ~9. The final solution was stirred for 2 h and aged for 2 h without stirring at room temperature. The solution was filtered and dried in an oven at 80˚C for 5 h. The prepared Pd/CeO_2 catalysts was calcined with air at 350, 550, 750, and 900˚C for 25 h, respectively. Bulk PdO was purchased from Sigma-Aldrich (99.97%). Similarly, various precious metals of Rh, Ru, Ir, and Pt were deposited on the CeO_2. Metal chloride precursors of $RhCl_3{\cdot}xH_2O$ (99.98%, Sigma-Aldrich), $IrCl_3{\cdot}xH_2O$ (≤100%, Sigma-Aldrich), $H_2PtCl_6{\cdot}6H_2O$ (≤100%, Sigma-Aldrich), and $RuCl_3$ (≤100%, Sigma-Aldrich) were used. Other metal oxide supports of TiO_2 (P25, Degussa), ZrO_2 (Sigma-Aldrich), and SiO_2 (Sigma-Aldrich) were also used instead of CeO_2 at otherwise the same synthesis conditions. Reaction, characterizations, and computational details can be found in supporting information.

Acknowledgements

This research was supported by the National Research Foundation of Korea (NRF-2016M3D3A1A01913255 and 2018R1A2A2A05018849). The experiments at PLS were supported in part by MSIP and POSTECH.

Keywords: methane, ethane, PdO, heterogeneous catalysis, oxidation

[1] a) P. Schwach, X. L. Pan, X. H. Bao, *Chem. Rev.* **2017**, *117*, 8497-8520; b) E. V. Kondratenko, T. Peppel, D. Seeburg, V. A. Kondratenko, N. Kalevaru, A. Martin, S. Wohlrab, *Catal. Sci. Technol.* **2017**, *7*, 366-381.

[2] P. Tomkins, M. Ranocchiari, J. A. van Bokhoven, *Acc. Chem. Res.* **2017**, *50*, 418-425.

[3] a) A. A. Latimer, A. R. Kulkarni, H. Aljama, J. H. Montoya, J. S. Yoo, C. Tsai, F. Abild-Pedersen, F. Studt, J. K. Norskov, *Nat. Mater.* **2017**, *16*, 225-229; b) M. Cargnello, J. J. D. Jaen, J. C. H. Garrido, K. Bakhmutsky, T. Montini, J. J. C. Gamez, R. J. Gorte, P. Fornasiero, *Science* **2012**, *337*, 713-717; c) Y. Lai, G. Veser, *Catal. Sci. Technol.* **2016**, *6*, 5440-5452; d) B. Xing, X. Y. Pang, G. C. Wang, *J. Catal.* **2011**, *282*, 74-82.

[4] a) K. T. Dinh, M. M. Sullivan, K. Narsimhan, P. Serna, R. J. Meyer, M. Dinca, Y. Román-Leshkov, *J. Am. Chem. Soc.* **2019**, *141*, 11641-11650; b) P. Tomkins, A. Mansouri, S. E. Bozbag, F. Krumeich, M. B. Park, E. M. C. Alayon, M. Ranocchiari, J. A. van Bokhoven, *Angew. Chem. Int. Ed.* **2016**, *55*, 5467-5471; c) K. Narsimhan, K. Iyoki, K. Dinh, Y. Román-Leshkov, *ACS Cent. Sci.* **2016**, *2*, 424-429; d) C. Hammond, M. M. Forde, M. H. Ab Rahim, A. Thetford, Q. He, R. L. Jenkins, N. Dimitratos, J. A. Lopez-Sanchez, N. F. Dummer, D. M. Murphy, A. F. Carley, S. H. Taylor, D. J. Willock, E. E. Stangland, J. Kang, H. Hagen, C. J. Kiely, G. J. Hutchings, *Angew. Chem. Int. Ed.* **2012**, *51*, 5129-5133.

[5] a) P. W. Wang, G. F. Zhao, Y. Wang, Y. Lu, *Sci. Adv.* **2017**, *3*; b) P. W. Wang, G. F. Zhao, Y. Liu, Y. Lu, *Appl. Catal. A* **2017**, *544*, 77-83.

[6] K. J. Chen, D. G. Madden, S. Mukherjee, T. Pham, K. A. Forrest, A. Kumar, B. Space, J. Kong, Q. Y. Zhang, M. J. Zaworotko, *Science* **2019**, *366*, 241-246.

[7] X. G. Guo, G. Z. Fang, G. Li, H. Ma, H. J. Fan, L. Yu, C. Ma, X. Wu, D. H. Deng, M. M. Wei, D. L. Tan, R. Si, S. Zhang, J. Q. Li, L. T. Sun, Z. C. Tang, X. L. Pan, X. H. Bao, *Science* **2014**, *344*, 616-619; b) P. F. Xie, T. C. Pu, A. M. Nie, S. Hwang, S. C. Purdy, W. J. Yu, D. Su, J. T. Miller, C. Wang, *ACS Catal.* **2018**, *8*, 4044-4048.

[8] Y. Kim, T. Y. Kim, H. Lee, J. Yi, *Chem. Commun.* **2017**, *53*, 4116-4119.

[9] a) M. Belgued, P. Pareja, A. Amariglio, H. Amariglio, *Nature* **1991**, *352*, 789-790; b) S. F. Moya, R. L. Martins, A. Ota, E. L. Kunkes, M. Behrens, M. Schmal, *Appl. Catal., A* ***2012****, 411, 105-113.*

[10] D. Soulivong, S. Norsic, M. Taoufik, C. Coperet, J. Thivolle-Cazat, S. Chakka, J. M. Basset, *J. Am. Chem. Soc.* ***2008****, 130, 5044-5045.*

[11] a) G. N. Li, L. Li, Y. Yuan, J. J. Shi, Y. Y. Yuan, Y. S. Li, W. R. Zhao, J. L. Shi, *Appl. Catal. B* **2014**, *158*, 341-347; b) Y. T. Chen, H. J. Zheng, Z. Guo, C. M. Zhou, C. Wang, A. Borgna, Y. H. Yang, *J. Catal.* **2011**, *283*, 34-44; c) L. H. Xiao, K. P. Sun, X. L. Xu, X. N. Li, *Catal. Commun.* **2005**, *6*, 796-801.

[12] R. J. Farrauto, J. K. Lampert, M. C. Hobson, E. M. Waterman, *Appl. Catal. B* **1995**, *6*, 263-270

[13] a) S. Colussi, A. Gayen, M. F. Camellone, M. Boaro, J. Llorca, S. Fabris, A. Trovarelli, *Angew. Chem. Int. Ed.* **2009**, *48*, 8481-8484; b) M. Danielis,

S. Colussi, C. de Leitenburg, L. Soler, J. Llorca, A. Trovarelli, *Angew. Chem. Int. Ed.* **2018**, *57*, 10212-10216.

[14] T. P. Senftle, A. C. T. van Duin, M. J. Janik, *ACS Catal.* **2017**, *7*, 327-332.

[15] Y. H. Chin, C. Buda, M. Neurock, E. Iglesia, *J. Am. Chem. Soc.* **2013**, *135*, 15425-15442.

[16] a) Y. Lou, J. Ma, W. D. Hu, Q. G. Dai, L. Wang, W. C. Zhan, Y. L. Guo, X. M. Cao, Y. Guo, P. Hu, G. Z. Lu, *ACS Catal.* **2016**, 6, 8127-8139; b) A. W. Petrov, D. Ferri, O. Kröcher, J. A. v. Bokhoven, *ACS Catal.* **2019**, 9, 2303–2312.

[17] a) J. S. Zou, Z. C. Si, Y. D. Cao, R. Ran, X. D. Wu, D. Weng, *J. Phys. Chem. C* **2016**, *120*, 29116-29125; b) X. L. Yang, M. M. Zhen, G. Li, X. Z. Liu, X. Y. Wang, C. Y. Shu, L. Jiang, C. R. Wang, *J. Mater. Chem. A* **2013**, *1*, 8105-8110.

[18] W. An, X. C. Zeng, C. H. Turner, *J. Chem. Phys.* **2009**, *131*. 174702.

[19] a) J. S. Lin, L. Y. Yang, T. Wang, R. X. Zhou, *Phys. Chem. Chem. Phys.* **2017**, *19*, 7844-7852; b) Y. Ryou, J. Lee, H. Lee, C. H. Kim, D. H. Kim, *Catal. Today* **2017**, *297*, 53-59.

Entry for the Table of Contents

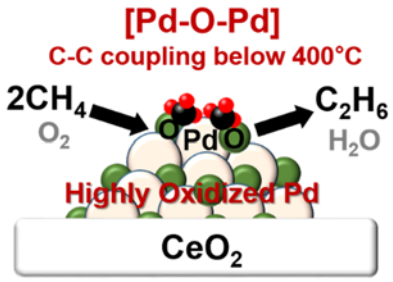

A highly oxidized Pd deposited on ceria could oxidize methane directly to ethane in a stable manner using gaseous O_2 below 400 ˚C. The Pd-O-Pd sites, not Pd-O-Ce, enabled the oxidative methane coupling.